NF-κB is a Central Regulator of Hypoxia-Induced Gene Expression

Dilem Shakir[1], Michael Batie[1], Chun-Sui Kwok[1]. Niall S. Kenneth[1], and Sonia Rocha[1]*

Department of Biochemistry, Cell and System Biology. Institute of Systems, Molecular and Integrative Biology, University of Liverpool. Liverpool L697ZB. United Kingdom.

*Corresponding author: Sonia Rocha, srocha@liverpool.ac.uk

Keywords: Hypoxia, NF-kappaB, RNA-seq, transcriptional repression

Abstract

Hypoxia is both a physiological and pathological signal in cells. Changes in gene expression play a critical role in the cellular response to hypoxia, enabling cells to adapt to reduced oxygen availability by regulating metabolism, angiogenesis, and survival pathways. These changes are primarily mediated by the HIF family of transcription factors, however other transcription factors such as NF-κB, are also activated in the hypoxic response. Although NF-κB is known to be activated under hypoxic conditions the extent of NF-κB contributions to the hypoxic response remains poorly understood. In this study we analyse hypoxia-induced NF-κB dependent gene expression, to define the NF-κB-dependent hypoxic signature. Our analysis reveals that a significant proportion of hypoxia-induced gene expression changes are NF-κB dependent, with majority of the hypoxia downregulated genes requiring NF-κB for their repression. We show that, while the NF-κB-mediated hypoxic response may vary between cell types, there are a core subset of hypoxia inducible genes that require NF-κB across multiple cell backgrounds. We demonstrate that NF-κB is critical for reactive oxygen species (ROS) generation and regulation of genes involved in oxidative phosphorylation under hypoxic conditions. This work highlights that NF-κB has a central role in hypoxia response, regulating a broader set of genes than previously thought, providing new understanding into the gene expression regulation by hypoxia and NF-κB.

Introduction

Hypoxia, or reduction in oxygen homeostasis, is both a physiological and pathological cue (Kaelin & Ratcliffe, 2008; Kenneth & Rocha, 2008; Xie & Simon, 2017). As oxygen is required for viability of many organisms, complex and intricate mechanisms have evolved for cells and organisms to be able not only to sense hypoxia, but to respond appropriately. These responses vary from increasing oxygen supply, to reducing oxygen consumption to eventual adaptation or cell death (Rocha, 2007). At the cellular level, the best understood response occurs via the transcription factor family, Hypoxia Inducible Factors (HIFs). HIFs are controlled by a family of 2-oxoglutarate dependent dioxygenases called Prolyl-hydroxylases (PHDs), that modify HIF, making a target for ubiquitylation via the von Hipple Lindau (VHL) containing E3-ligase complex and destruction by the 26S proteosome (An & Rettig, 2005; Bruegge *et al*, 2007; Fandrey *et al*, 2006). In addition to HIF, other transcription factors are also activated in response to hypoxia, including the NF-κB family of transcription factors (Cummins & Taylor, 2005; Kenneth & Rocha, 2008) NF-κB is best known for its role in innate immunity and its response and control of inflammation, but is also activated in response to physical, physiological and oxidative stresses (Perkins & Gilmore, 2006). NF-κB is a family of homo and heterodimers of 5 genes producing 7 proteins, RelA, RelB, cRel, p105 and p50, and p100 and p52 (Perkins & Gilmore, 2006). Their regulation occurs at several levels from transcription to post-translational modifications and also cytoplasmic sequestration via their interaction with a family of inhibitors, called Inhibitors of κB, or IκBs (Perkins & Gilmore, 2006). Given its complexity, NF-κB targets are numerous and can also be characterised based on their timing of expression, such as early, mid and late genes (Tian *et al*, 2005). Furthermore, it is under several positive and negative feedback loops depending on the activation stimulus, including NF-κB subunits themselves, IκBs, and upstream activators and regulators (Prescott *et al*, 2021). NF-κB is activated by almost all stresses investigated so far but are best characterised following infection with bacteria or virus, or in response to pro-inflammatory cytokines recognised by members of the tumour necrosis factor receptor superfamily (TNFRSF) (Perkins, 2007). Receptor activation initiates a signalling cascade involving the IκB kinase (IKK) complex that phosphorylates IκB, leading to its degradation and the release of NF-κB for nuclear translocation and gene transcription (Adhikari *et al*, 2007). Many more levels of complexity and control exist in the NF-κB pathway, making it one of the most complex transcription factors to study. However, its importance is well established in essential aspects such as immunity, response to inflammation, cell death, proliferation and DNA damage responses (Almaden *et al*, 2016; Gerondakis & Siebenlist, 2010; Liu *et al*, 2017; Qin *et al*, 2007; Volcic *et al*, 2012; Xia *et al*, 2018; Xu *et al*, 2015). NF-κB activation in response to hypoxia has been observed by several studies, including some of our own (Al-Anazi *et al*, 2018; Culver *et al*, 2010; D'Ignazio *et al*, 2017; D'Ignazio & Rocha, 2016; Melvin *et al*, 2011; Patel *et al*, 2017). While the exact mechanism of activation slightly differs from study to study, it is well established that hypoxia-dependent activation of NF-κB requires IKK activation, and this has been seen in the fruit fly, mouse and human cells (Culver

et al., 2010). Additional mechanistic insights include requirement of calcium release to activate IKK upstream kinase (Culver *et al.*, 2010), Transforming Growth Factor Activated Kinase (TAK1) (Adhikari *et al.*, 2007; Melvin *et al.*, 2011), input from PHD enzymes (Wilson *et al*, 2020) and lack of IκB degradation (Culver *et al.*, 2010).

It is well established that cells have a specific transcriptional response to hypoxia, and analysis of several RNA-sequencing datasets revealed a conserved hypoxia inducible signature (Puente-Santamaria *et al*, 2022). There is also a recognised set of genes that are repressed in response to hypoxia, but the mechanisms controlling this are far less understood (Batie *et al*, 2018; Cavadas *et al*, 2017). However, whether the NF-κB response to hypoxia is a general feature of most cells, or if there is a common gene expression signature, it is not known. Here we combined analysis of publicly available datasets across different cellular backgrounds, with transcriptomics analysis of siRNA mediated depletion of NF-κB subunits in hypoxia to uncover the NF-κB contribution to the cellular response. Our analysis shows NF-κB is required for activation of a subset of hypoxia activated genes (i.e., 30%) but strikingly is required for the repression of around 60% of hypoxia repressed genes. Furthermore, our analysis reveals a wide spread of NF-κB dependent hypoxia induced genes as being hypoxia regulated across all cell types analysed, with some cell type specificity. Interestingly, most of the genes were previously not known to dependent on NF-κB to be regulated in hypoxia, and only a small subset is recognised NF-κB target genes, demonstrating the context dependent nature of NF-κB. Lastly, we demonstrate that NF-κB is required to maintain reactive oxygen levels necessary for cell signalling.

Methods

Cell culture

Human cervical carcinoma HeLa, lung carcinoma A549, brain glioblastoma U87, and breast adenocarcinoma MCF-7 cell lines were obtained from the American Type Culture Collection (ATCC, USA) and maintained at 5% CO_2 and 37°C in Dulbecco's modified Eagle's medium (DMEM) supplemented with 10% v/v foetal bovine serum (FBS), 1% L-glutamine (Lonza, UK), and 1% penicillin-streptomycin (Lonza, UK). Cell lines were cultured not more than 30 passages and routinely tested for mycoplasma contamination using MycoAlert Mycoplasma Detection Kit (Lonza, UK).

Hypoxia treatments and siRNA transfections

Hypoxia treatments were performed by incubating cells in an InVivo300 Hypoxia Workstation (Baker Ruskin, UK) at 1% O_2, 5% CO_2 and 37°C. Cells were transfected with 27 nM of small interfering RNA (siRNA) oligonucleotides (Eurofins Genomics, Germany) for 48 h using Interferin (Polyplus, France) transfection reagent according to manufacturer's instructions. The following oligonucleotide sequences were used for siRNA knockdowns: Control CAGUCGCGUUUGCGACUGG RelA

GCCCUAUCCCUUUACGUCA, RelB GGAUUUGCCGAAUUAACAA, cRel ACAGCUGAAUGAUAUUGAA.

RNA extraction and RNA-seq data analysis

RNA was extracted using the RNeasy Mini Kit (Qiagen, UK) following manufacturer's instructions. RNA-seq was performed on a Novaseq 6000 (Illumina, UK) with paired end 150 bp run type. Sequencing reads were aligned to the human genome assembly version hg38 (GRCh38, Ensemble) using STAR sequence aligner (Dobin *et al*, 2013) to generate coordinate-sorted binary alignment map (bam) files. Read counts for each transcript (GRCh38, Ensembl) were generated using the featureCounts function of Subread (Liao *et al*, 2013). Differential expression analysis was performed using R Bioconductor package DESeq2 (Love *et al*, 2014) with filtering for effect size (>±0.58 $\log_2$ fold change) and statistical significance (FDR <0.05). Sample to sample distance comparison heatmaps using rlog transformed read count data were generated using R Bioconductor packages DESeq2 and pheatmap. PCA plot of rlog transformed read count data were generated using R Bioconductor packages DESeq2 and ggplot2. Volcano plots for display of differential expression analysis were generated using R Bioconductor package EnhancedVolcano. Z-score heatmaps of VST transformed read count data were generated using DESeq2 and pheatmap. Overrepresentation analysis (ORA) was performed using WEB-based Gene SeT AnaLysis Toolkit (WebGestalt) (Liao *et al*, 2019) in overrepresentation analysis (ORA) mode using the Molecular Signatures Database (MSigDB) hallmark gene sets (Liberzon *et al*, 2015; Subramanian *et al*, 2005). Motif enrichment analysis was performed using the findMotifs tool of HOMER (Heinz *et al*, 2010) with gene promoters defined as 400 bps upstream to 100 bps downstream of transcription start sites.

qPCR

RNA was extracted using the RNeasy Mini Kit (Qiagen, UK) following manufacturer's instructions. RNA was converted to cDNA using iscript reverse transcription kit (Bio-Rad) and qPCR analysis of transcript expression changes was performed by running 3 µl of DNA on a QuantStudio 1 qPCR platform (Applied Biosystems) with power-track Sybr green reaction mix (Applied Biosystems) in a final reaction of 15 µl. The following qPCR primers were used: Actin F CTGGGAGTGGGTGGAGGC and R TCAACTGGTCTCAAGTCAGTG, 18S F AAACGGCTACCACATCCAAG and R CGCTCCCAAGATCCAACTAC, CA9 F CTTTGCCAGAGTTGACGAGG and R CAGCAACTGCTCATAGGCAC, RelA F CTGCCGGGATGGCTTCTAT and R CCGCTTCTTCACACACTGGAT, RelB F TCCCAACCAGGATGTCTAGC and R AGCCATGTCCCTTTTCCTCT, cRel F CTGCCTTCTTCAAGCTGGTC and R CGCTTCCATTCCGACTATGT, GADD45B F TCGGCCAAGTTGATGAATG and R TGAGCGTGAAGTGGATTTG, JUNB F GACCAAGAGCGCATCAAA and R TCTTCACCTTGTCCTCCA, NFIX F TGTTGATGACGTGTTCTATCC and R

CCAGCTTTCCTGACTTCTTTA, USP28 F GAAGTAGAGGAGTGGGAAGA and R GAAGGCTCTTGTGATGTAGAG, KMT2E F GCCAACTGCCCTACATAAA and R GCTCTTTACCCAGGAAGAATAC, TGFA F GCATGTGTCTGCCATTCT and R GTGATGGCCTGCTTCTTC, VIM F CCAGCTAACCAACGACAAA and R TCCTCTCTCTGAAGCATCTC, SAP30 F GAGCGCAAGGCATCTTTA and R AATCACCTCCATCATCATCAC, EGLN3 F CTACGTCAAGGAGAGGTCTAA and R CAGATAGTAGATGCAGGTGATG, KLF10 F TGCCTTCGTGTTGAAATCC and R GGGCGCGATTATGCAATTA, BCL3 F CTCTCCATATTGCTGTGGTG and R TGTCTGCCGTAGGTTGT, FTH1 F AGTGCCGTTGTTCAGTTC and R AGACAGCCACACCTTAGT, GCLM F CTGTTCAGTCCTTGGAGTTG and R CTCCCAGTAAGGCTGTAAATG, NQO1 F CCTGGAAGGATGGAAGAAAC and R GAATCCTGCCTGGAAGTTTAG, AIFM1 F CCAGCCACCTTCTTTCTATG and R CCATGTTGTCTCTCACATCC, IDH1 F GCAGTACAAGTCCCAGTTT and R TGAAGCCTCCCTCTGATT, SOD1 F TCGAGCAGAAGGAAAGTAATG and R CCTGCTGTATTATCTCCAAACT, CCND3 F GATTTCCTGGCCTTCATTCT and R GGGTACATGGCAAAGGTATAA, CASP10 F CGTATCAAGGAGAGGAAGAAC and R TGTGGCTCTGTTACCATTAC, LAMTOR2 F CACCCTGCTGCTGAATAA and R CCCAGATGTTACTGGCTATG.

Statistical analysis

For qPCR analysis comparing two conditions, statistical significance was determined via Student's t-test. For qPCR analysis comparing more than two conditions, statistical significance was determined via one-way ANOVA with post-hoc Dunnett's test. For overlap of differentially expressed genes (DEGs) identified by RNA-seq, statistical significance was determined via hypergeometric test using Venn diagram function of an online data analysis tool with its default parameters (Iqbal, 2021). For all other statistical analysis, default settings of the analysis tool were used. In all cases, *$P < 0.05$, **$P < 0.01$, ***$P < 0.001$.

Data mining of publicly available datasets

HeLa HIF ChIP-seq dataset (Ortmann *et al*, 2021) (GSE169040) was downloaded from the Gene Expression Omnibus (Edgar *et al*, 2002). MCF-7 (GSE153291), A549 (GSE186370), HCT116 (GSE81513), U87 (GSE78025), and 501-MEL (GSE132624) hypoxia RNA-seq datasets and the HEK293FT siSENP3 RNA-seq dataset (Zhou *et al*, 2023) (GSE197030) were downloaded from the Gene Expression Omnibus (Edgar *et al.*, 2002) and processed using the RNA-seq data analysis pipeline described above. NF-κB target genes were downloaded from the Gilmore laboratory website

<https://www.bu.edu/nf-kb/gene-resources/target-genes/> and converted to Ensembl gene annotation format using R Bioconductor package biomaRt (Durinck *et al*, 2005).

Cellular Reactive Oxygen Species detection

Cells were fixed and cellular reactive oxygen species (ROS) were measured using CellROX Green reagent (ThermoFisher) according to the manufacturer's instructions. Cells were imaged using an Epifluorescence microscopy (Zeiss Axio Observer Z.1). Images were quantified using OMERO open microscopy environment (Allan *et al*, 2012). Scale bars = 20µm.

Immunoblots

Cells were lysed in Radio Immunoprecipitation Assay (RIPA) lysis buffer (50 mM Tris-HCl pH 8.0, 150 mM NaCl, 1% v/v NP40, 0.25% w/v Na-deoxycholate, 0.1% w/v SDS, 10 mM NaF, 2 mM Na3VO4, and 1 tablet protease inhibitor (Thermo Fisher Scientific) per 10 mL of lysis buffer). Cells containing the lysis buffer scraped into Eppendorf tubes and incubated on ice for 10 minutes to complete the lysis process. The samples were centrifuged for 15 minutes at 13,000 rpm, 4°C. The supernatant was collected, and protein concentration of cell lysates were determined using Bradford assay (BioRad). Cells treated with hypoxia were harvested in the hypoxia chamber to prevent reoxygenation. 20 µg of protein was prepared in 2× SDS loading buffer (100 mM Tris-HCl pH 6.8, 20% v/v glycerol, 4% w/v SDS, 200 mM DTT and Bromophenol Blue). SDS-PAGE and immunoblots were carried out using standard protocols. The following primary antibodies were used for immunoblotting: RelA (sc-8008, Santa Cruz), RelB (10544, Cell Signalling), cRel (4727, Cell Signalling), HIF-1α (610958, BD Biosciences), β-Actin (66009-1-lg, Proteintech), IDH1 (12332-1-AP, Proteintech), SOD1 (sc-17767, Santa Cruz), Total Oxphos Antibody Cocktail for detecting ATP5A, UQCRC2, and SDHB (ab110411, abcam). ImageJ was used for quantification of immunoblots with band intensities normalised to β-Actin.

Results

Transcriptional response profile of hypoxia stimulation is NF-κB dependent.

As the majority of NF-κB target genes have been characterised in the context of inflammatory signalling, we aimed to determine the contribution NF-κB to the transcriptional response to hypoxia within a given cell type. As such, to identify the hypoxia inducible NF-κB dependent gene signatures, an unbiased high-throughput RNA-sequencing (RNA-seq) analysis was performed. HeLa cells were transfected with control siRNA or NF-κB subunits, RelA, RelB or cRel siRNAs and exposed to 21% O_2 (normoxia) or 1% O_2 (hypoxia) for 24 hours (h) prior to profiling for global transcriptomic analysis using RNA-seq (Figure 1A). Principal component analysis of the collected RNA-seq data showed that samples cluster by condition (Sup. Figure S1A). Control samples treated with normoxia clustered together with relatively weak correlation to the rest of the samples, while hypoxia treated samples were

grouped close to one another, with the exception of siRelA treated samples (Sup. Figure S1A). Also, close clustering of replicates within each condition demonstrates their relative similarity to each other. In this analysis, efficiency of the hypoxia stimulation was investigated using DESeq2 normalised counts acquired from RNA-seq analysis showing differential expression of the gene in hypoxia samples, compared to normoxia, as expected the expression of Carbonic Anhydrase (*CA9*), a core hypoxia upregulated gene, was increased in response to hypoxia (Sup. Figure S1B). Additionally, DESeq2 normalised counts of *RelA*, *RelB*, and *cRel* were reduced by the respective siRNA treatments, demonstrating efficient siRNA depletion (Sup. Figure S1C-E). To investigate the gene expression changes with hypoxia stimulation between individual NF-κB subunit depletions, volcano plots were generated following differential expression analysis by comparing each condition to normoxia control (Figure 1B-E). This analysis revealed that more than 2,000 genes were differentially expressed at 5% false discovery rate (FDR) and log2 fold change 0.58 in hypoxia control siRNA treated samples compared to normoxia control siRNA treated samples (Figure 1B, Dataset S1). Overall, RelA depletion with hypoxia exposure induced the highest transcriptional changes, followed by RelB or cRel depletions with hypoxia stimulation (Figure 1C-E, Dataset S1). When we compared the effect of individual NF-κB subunits in hypoxia inducible gene signatures, all three subunits showed a shared proportion of genes between each other, while also having high portion of genes regulated by RelA, RelB or cRel, exclusively (Figure 1F-G, Dataset S1).

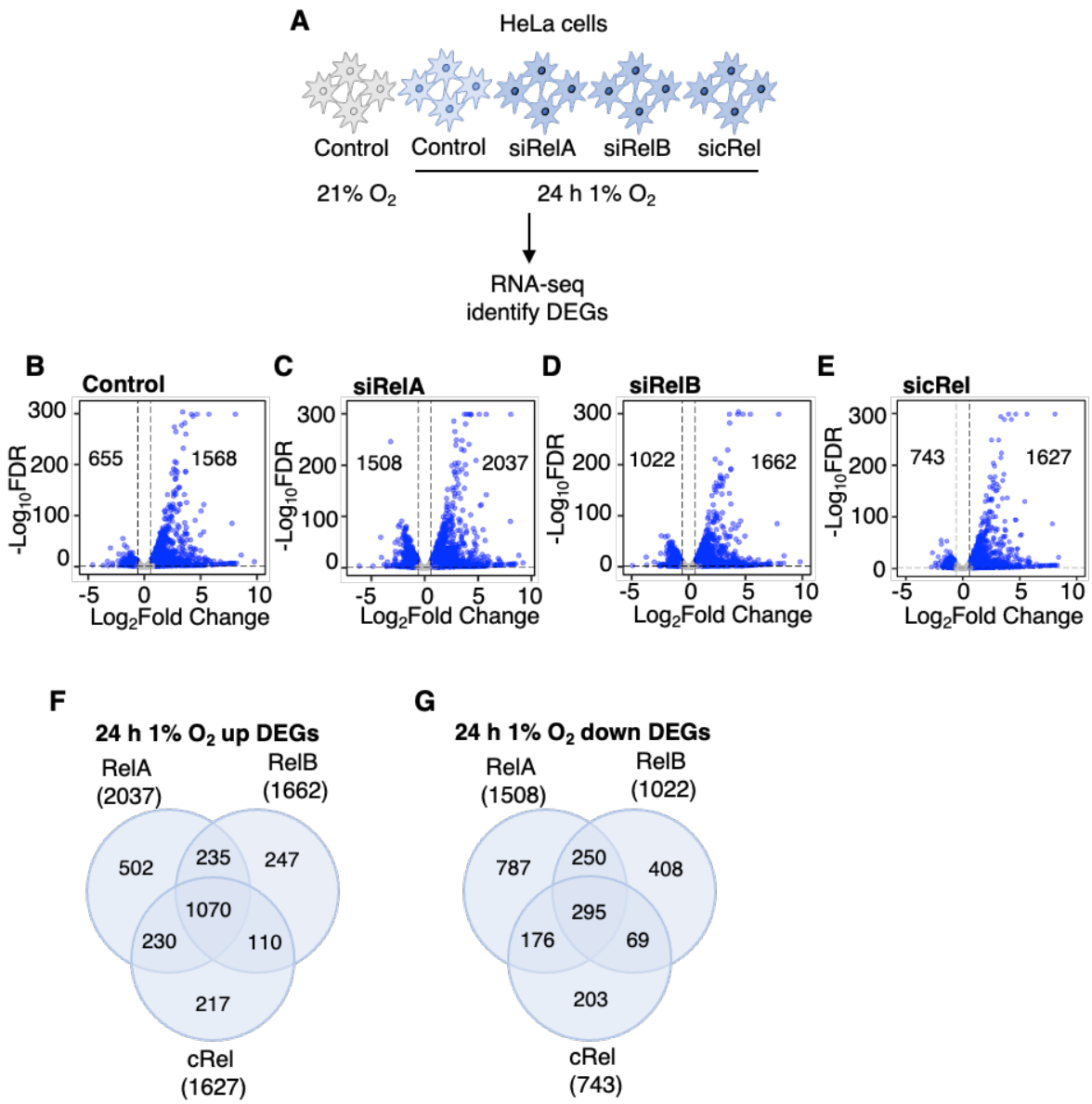

Figure 1. Gene expression changes in response to hypoxia and NF-κB subunit depletions in HeLa cells. **A.** RNA-seq (n=2) in HeLa cells cultured at 21% oxygen (normoxia) or exposed to 24 h 1% oxygen (hypoxia), transfected with control siRNA or RelA, RelB or cRel siRNAs. **B-E.** Differential expression analysis volcano plots for 24 h hypoxia control, siRelA, siRelB or sicRel compared to normoxia control. Blue points indicate DEGs. **F-G.** Overlap of siRelA, siRelB and sicRel upregulated genes in hypoxia, compared to normoxia control (**F**) and siRelA, siRelB and sicRel downregulated genes in hypoxia, compared to normoxia control (**G**) in HeLa cells.

To identify the NF-κB-dependent, hypoxia-inducible gene signatures of the obtained data, we performed integrative analysis, comparing the list of hypoxia differentially regulated genes with the combined list of NF-κB subunits depleted, differentially hypoxia regulated genes. Overlap analysis revealed that 35.5% (556 out of 1568) of the hypoxia upregulated genes (Figure 2A), and 62.6% (410 out of 655) of the hypoxia downregulated genes were NF-κB-dependent (Figure 2B). Overall, this analysis highlights the importance of NF-κB in the regulation of the transcriptional response to hypoxia.

Furthermore, the heatmap generated using the NF-*κ*B dependent hypoxia up- and down-regulated genes showed that individual NF-*κ*B subunit depletions displayed different transcriptional profiles (Figure 2C). We also investigated the number of shared genes by the different Rel subunits, revealing that although 41 genes were simultaneous dependent on all NF-κB subunits for hypoxia upregulation, most of the other genes were regulated by individual subunits (Figure 2D; Dataset S2). Similar results were also obtained for repressed genes in hypoxia (Figure 2E; Dataset S2). This analysis revealed RelB dependent hypoxia regulated genes have the highest proportion followed by cRel and RelA.

To characterise the identified NF-*κ*B dependent hypoxia inducible gene signatures, their association with hallmark gene sets was investigated. Hypoxia, glycolysis, and TNF-α signalling via NF-*κ*B are the top three gene signatures significantly enriched at RelA-dependent 24 h hypoxia up-regulated DEGs. RelB-dependent 24 h hypoxia up-regulated DEGs are enriched in Epithelial–mesenchymal transition (EMT) and myogenesis gene signatures. Finally, EMT, TNF-α signalling via NF-*κ*B, and inflammatory response are the top three gene signatures significantly enriched at cRel-dependent 24 h hypoxia up-regulated DEGs (Figure 2F). Oxidative phosphorylation and ROS gene sets are significantly enriched at RelA-, RelB- and cRel-dependent 24 h hypoxia down-regulated DEGs (Figure 2G). Next, we determined if NF-*κ*B subunits had been found at the promoters of hypoxia regulated genes. To this end, we took advantage of the ChIP-Atlas database (Zou *et al*, 2024). This analysis revealed significant enrichment of RelA (80%) but also RelB (22%) and cRel (18%) in both hypoxia upregulated and downregulated genes (Figure 2H), indicating at least a subset of the NF-*κ*B dependent hypoxia inducible genes are directly regulated by NF-*κ*B. We also confirmed that some of the NF-*κ*B dependent hypoxia regulated genes have been previously described as direct NF-*κ*B targets in the Gilmore database (Sup. Figure S2A), however this is only a subset of the genes we identified.

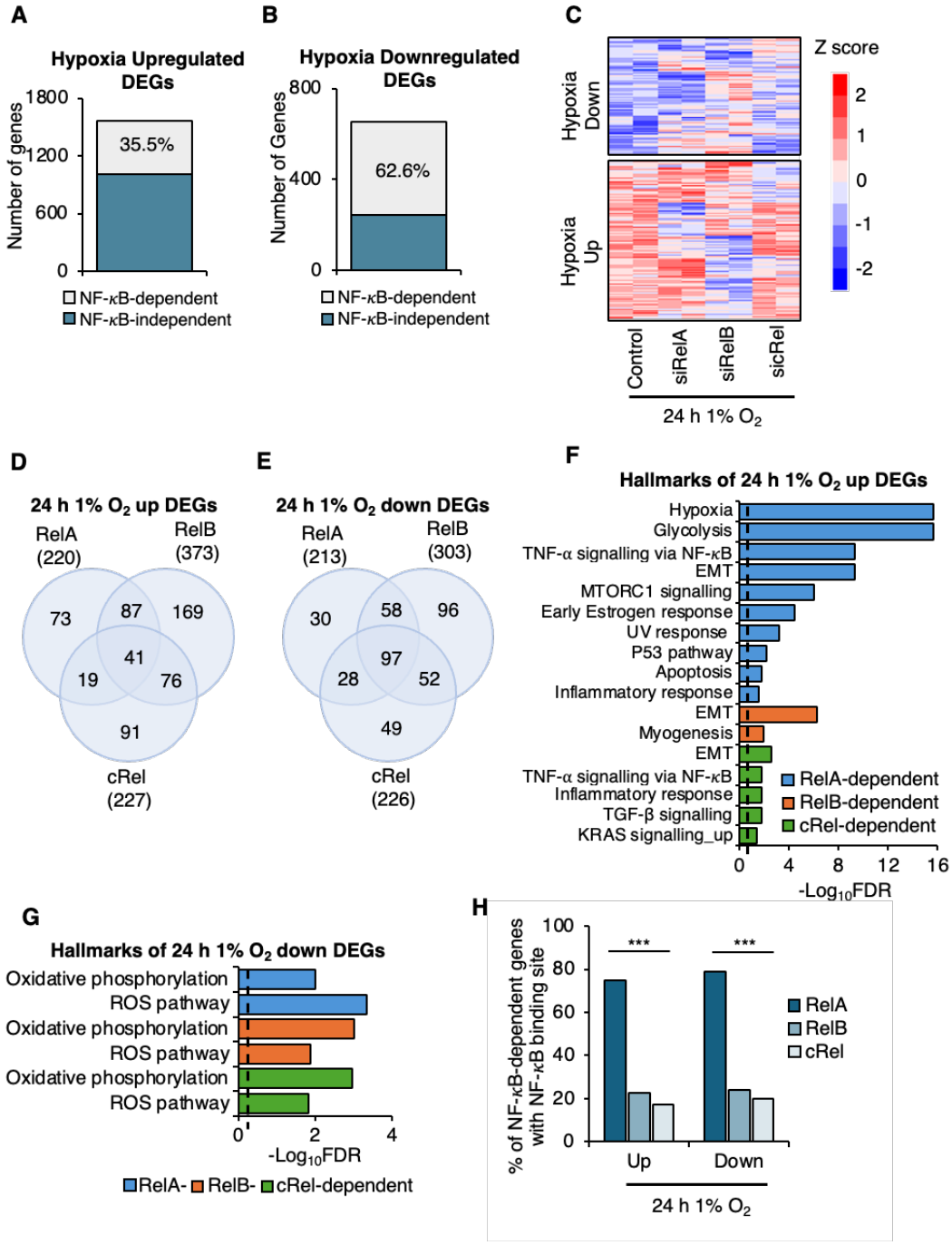

Figure 2. NF-κB is required for 35% of hypoxia induced genes and 63% of hypoxia repressed genes.
A-B. NF-κB dependence of hypoxia inducible Differential Expressed Genes (DEGs); percentage of NF-κB dependent DEGs are labelled. **C.** Heatmap displaying Z score transformed gene expression levels for NF-κB dependent hypoxia regulated genes. **D-E.** Overlap of RelA, RelB or cRel-dependent hypoxia up- or down-regulated DEGs. **F-G.** Over Representation Analysis (ORA) was performed through WEB-based Gene SeT AnaLysis Toolkit using the Molecular Signatures Database hallmark gene sets, investigating NF-κB dependent hypoxia upregulated DEGs (**F**) or downregulated DEGs (**G**). Dashed line shows statistical significance threshold of FDR 0.05 ($-Log_{10}FDR$ 1.3). (**H**) Overlap of NF-κB dependent hypoxia up- and down-regulated DEGs identified by RNA-seq (n=2) with NF-κB subunit binding sites acquired from ChIP-seq Atlas database. Percentage of DEGs containing an NF-κB subunit binding site are displayed; statistical significance of the gene list overlaps was determined via hypergeometric test, *** $P < 0.001$.

Motif enrichment analysis shows HIF-1α and HIF-1β motifs are enriched at RelA- and RelB-dependent 24 h hypoxia up-regulated DEGs (Sup. Figure S2B), and HIF-2α and HIF-1β motifs are enriched at cRel-dependent 24 h hypoxia up-regulated DEGs (Sup. Figure S2B), suggesting a role of HIF subunits in NF-κB controlled gene expression increases in hypoxia. The motif enrichment analysis of each NF-κB subunit-dependent hypoxia down-regulated DEGs show a variety of known NF-κB associated transcription factors (Sup. Figure S2C), indicating distinct transcriptional regulation of RelA, RelB and cRel dependent hypoxia down-regulated gene signatures. To further elucidate the correlation of NF-κB controlled hypoxic gene expression changes with HIF binding sites, we analysed publicly available HIF subunit ChIP-seq datasets in HeLa cells exposed to hypoxia (Sup. Figure S3A-C). Similar to motif enrichment analysis, HIF subunit (HIF-1α, HIF-2α and HIF-1β) binding sites are enriched at RelA-, RelB-, and cRel-dependent 24 h hypoxia up-regulated DEGs, but not at RelA-, RelB-, and cRel-dependent 24 h hypoxia down-regulated DEGs, further indicating HIF involvement in NF-κB dependent hypoxia induced gene activation.

NF-κB dependent hypoxia inducible gene expression changes are also observed by qPCR.

To validate the obtained data from the RNA-seq analysis, we selected several genes with high log2 fold change in hypoxia compared to normoxia, and some known HIF and/ or NF-κB target genes amongst the 556 NF-κB dependent hypoxia up-regulated genes (*BCL3*, *KMT2E*, *SAP30*, *TGFA*, *EGLN3*, *USP28*, *VIM*, *NFIX*, *GADD45B*, *JUNB*, *KLF10*, *FTH1*) and 410 NF-κB dependent hypoxia down-regulated genes (*GCLM*, *CCND3*, *NQO1*, *AIFM1*, *SOD1*, *CASP10*, *LAMTOR2*, *IDH1*) to analyse by quantitative polymerase chain reaction (qPCR) (Figure 3A, Sup. Table S1). HeLa cells were transfected with control siRNA or NF-κB subunits, RelA, RelB, or cRel siRNAs and exposed or not to 24 h hypoxia prior to qPCR analysis. In this analysis, efficiency of the hypoxia stimulation was measured using *CA9* (Sup. Figure S4A), as expected expression of this gene was highly upregulated in response to hypoxia. Additionally, RNA levels of *RelA*, *RelB*, and *cRel* were reduced by in response to their respective siRNA treatments, demonstrating robust siRNA depletion (Sup. Figure S4B-D). RNA levels of all the selected NF-κB dependent hypoxia upregulated genes were significantly increased in hypoxia control siRNA treated samples compared to normoxia control siRNA treated samples (Figure 3B-D). Next, effect of the NF-κB subunits was tested individually on hypoxia up- and down-regulated gene expression changes. As a result, *USP28*, *VIM*, *NFIX*, and *FTH1* significantly decreased following RelA depletion in hypoxia compared to hypoxia control sample (Figure 3B). Also, *BCL3* showed a slight decrease with RelA depletion in hypoxia, however this result is not statistically significant (Sup. Figure S4E). *KMT2E* levels were not altered by RelA depletion (Sup. Figure S4E). All the selected RNA-seq RelB dependent hypoxia-upregulated genes, *USP28*, *VIM*, *NFIX*, *SAP30*, *TGFA*, and *EGLN3*, significantly decreased following RelB depletion in hypoxia compared to hypoxia control sample (Figure 3C). Similarly, *USP28*, *FTH1*, and *JUNB* significantly decreased following cRel depletion in

hypoxia compared to hypoxia control sample (Figure 3D). *GADD45B* showed a slight decrease with cRel depletion in hypoxia, however this result was not statistically significant (Sup. Figure S4F). *KLF10* was not responsive to cRel depletion (Sup. Figure S4F). In summary, 5 out of 6 RelA dependent hypoxia up-regulated genes, 6 out of 6 RelB dependent hypoxia-up-regulated genes, and 4 out of 5 cRel dependent hypoxia up-regulated genes were successfully validated by qPCR (Figure 3B-D). RNA levels of the selected RNA-seq NF-κB dependent hypoxia down-regulated genes significantly decreased in hypoxia control siRNA treated samples compared to normoxia control siRNA treated samples (Figure 3E-F). Following siRNA depletion of RelA, *GCLM* and *IDH1* significantly increased expression in hypoxia compared to hypoxia control (Figure 3E). Similarly, RelB depletion followed by hypoxia exposure, increased the mRNA expression of *GCLM*, *IDH1*, *AIFM1*, *CCND3*, and *CASP10*, compared to hypoxia control (Figure 3F). *SOD1* slightly increased with RelB depletion in hypoxia, however this result is not significant (Sup. Figure S4G). None of the selected cRel dependent hypoxia downregulated genes were affected by cRel depletion in hypoxia, except *SOD1*, which cRel depletion shows the opposite effect of obtained in the RNA-seq analysis (Sup. Figure S4H). Also, LAMTOR2 was predicted to be both RelB and cRel dependent hypoxia regulated gene, however RelB or cRel depletion shows no effect on its mRNA expression, maintaining a decreased expression level following hypoxia stimulation (Sup. Figure S4G-H). In conclusion, 5 out of 7 RelB dependent, and 2 out of 2 RelA dependent hypoxia down-regulated genes were successfully validated by qPCR, however none of the selected RNA-seq cRel dependent genes had an effect on reversing the impact of hypoxia stimulation on the gene expressions. This indicates that RelA and RelB have a more dominant role on hypoxia down-regulated genes, compared to cRel.

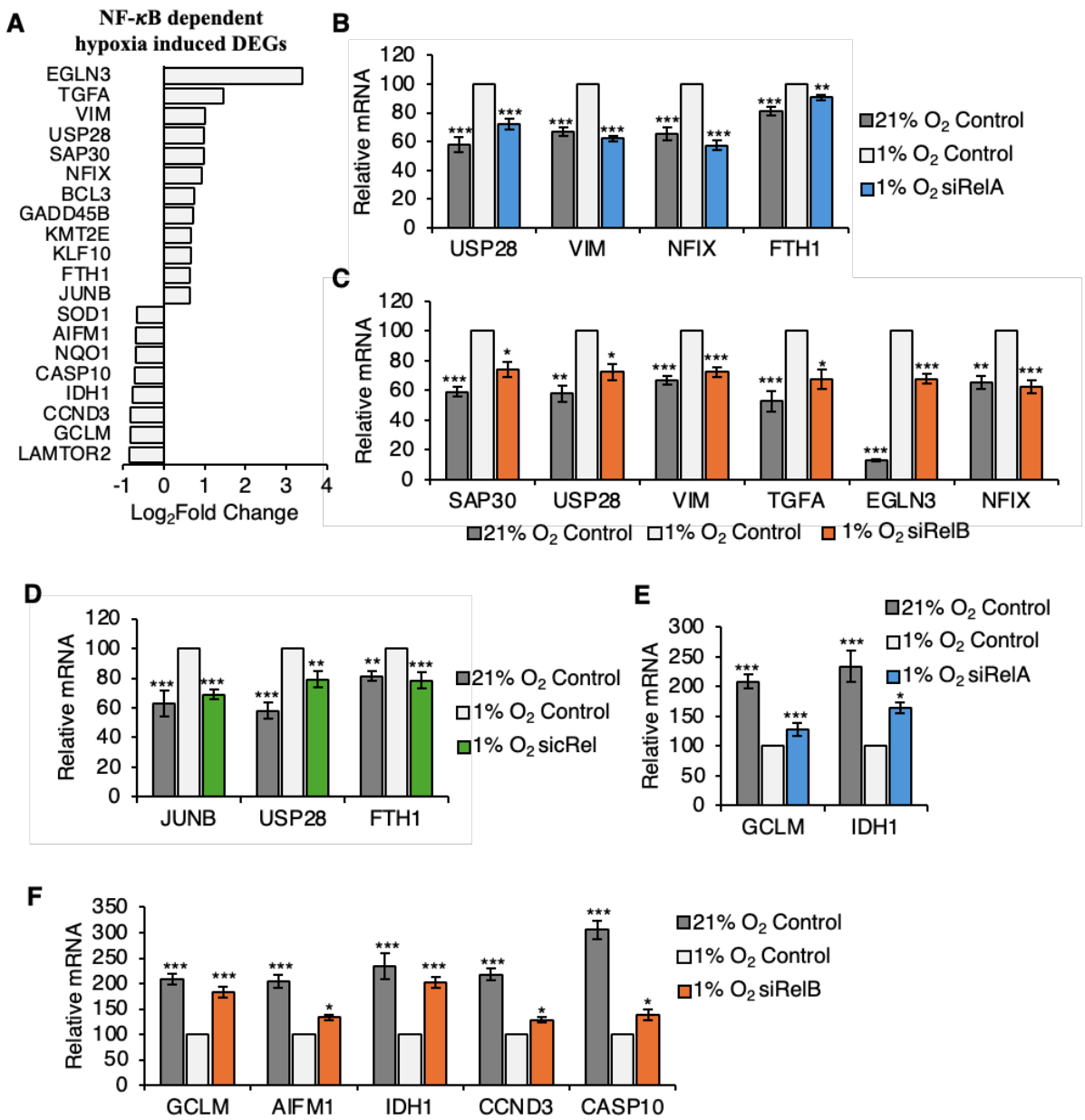

Figure 3. Validation of NF-κB dependent hypoxia inducible gene expression changes in HeLa cells.
A. Log_2Fold change of selected NF-κB dependent hypoxia up- and down-regulated DEGs showing altered transcript levels in hypoxia compared to normoxia identified by RNA-seq (n=2). **B-F.** qPCR analysis in HeLa cells cultured at 21% oxygen (control) or 24 h 1% oxygen (hypoxia), transfected with control siRNA or RelA, RelB or cRel siRNAs. RelA- (**B**), RelB- (**C**), and cRel-dependent (**D**) hypoxia upregulated DEGs. RelA- (**E**) and RelB-dependent (**F**) hypoxia downregulated DEGs. Relative mRNA expression levels of the indicated genes were analysed using 18S as a normalising gene. Graphs show mean (n=4) ± SEM, * $P < 0.05$, ** $P < 0.01$, *** $P < 0.001$. Statistical significance was determined via one-way ANOVA with post-hoc Dunnett's test.

NF-κB controlled hypoxia gene signatures in other cell types.

Given that we had uncovered a variety of genes that are dependent on NF-κB for the response to hypoxia in HeLa cells, we wanted to examine if these genes are also hypoxia regulated in other cell types. To address this question, we analysed hypoxia RNA-sequencing data in human cancer cell lines across different tissues, A549 (lung carcinoma), U87 (glioblastoma), HCT-116 (colorectal carcinoma), MCF-

7 (breast adenocarcinoma), 501-mel (melanoma metastasis) and SKNAS (neuroblastoma) (Figure 4A) (Sup. Table S2-3). Following quality control and the analysis pipeline (Sup. Figure S5A), volcano plots were created demonstrating the differential expressed genes (DEGs) that were significantly changed, both upregulated or downregulated across each cell line in response to hypoxia (Figure 4B). Comparing these hypoxia gene signatures across different cell backgrounds with our HeLa derived NF-κB dependent hypoxia signature revealed varying degrees of overlap, with very high presence in cells such as U87, HCT-116 and MCF-7 and more modest in SKNAS cells, across all NF-κB subunits (Figure 4C; Sup. Figure S6A). We also confirmed that a subset of these genes has been previously described as direct NF-κB target genes in the Gilmore database (Figure 4D; Sup. Figure S6B). Finally, we were able to validate by qPCR analysis the vast majority of the NF-κB dependent control over selected genes in U87, MCF-7 and A549 cells (Figure 5B-L; Sup. Figure S7A-F; Sup. Figure S8A-C; Sup. Figure S9A-S; Sup. Table S1). Once again, RelB seems to have the most widespread impact of hypoxia dependent gene changes across all the cell systems investigated (Figure 5B-L). Furthermore, some are also dependent on RelA, and very few are controlled by cRel (Figure 5B-L). Taken together these data indicate that role of NF-κB in controlling gene expression is conserved across a variety of cell lines.

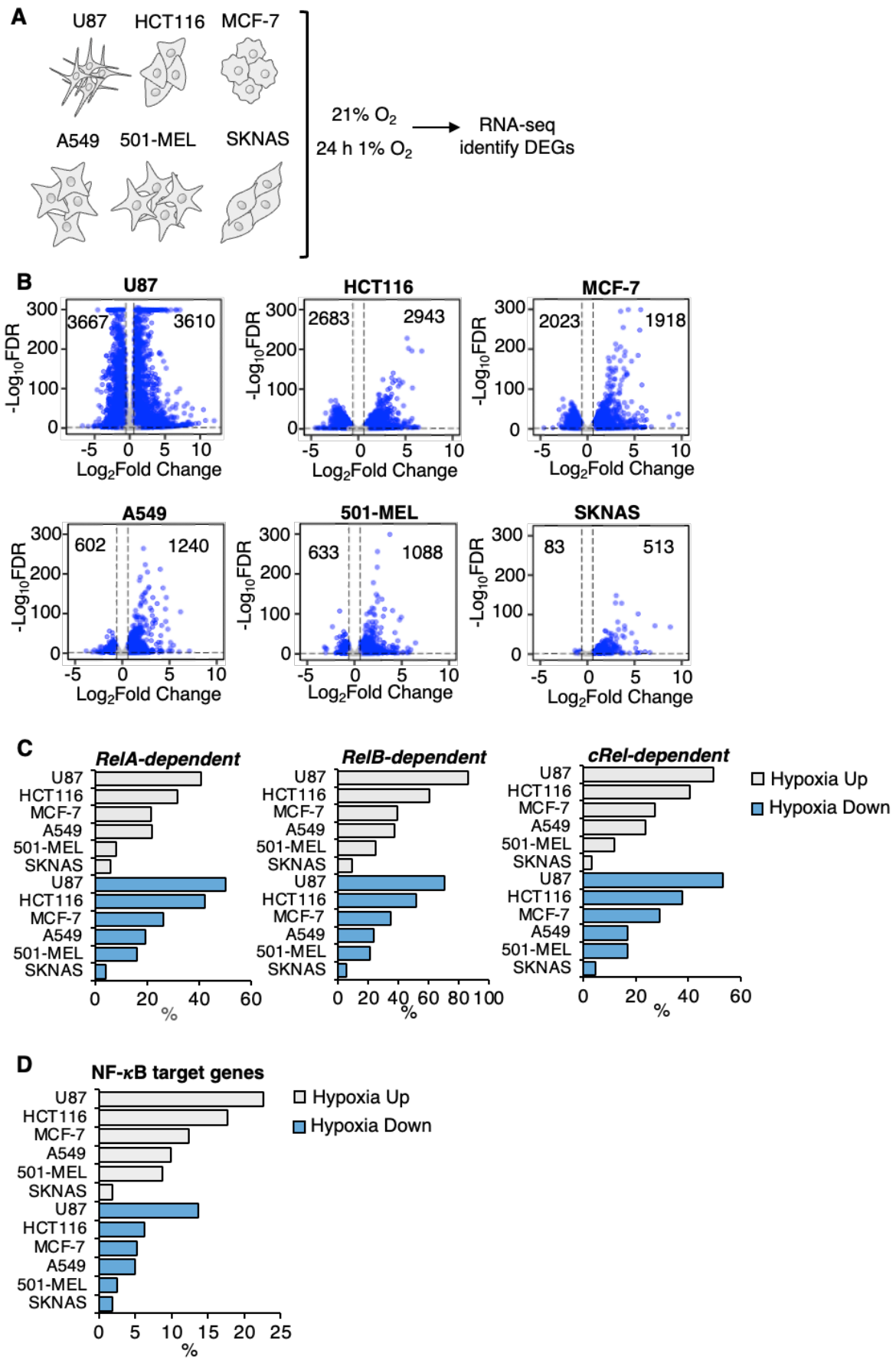

Figure 4. Identification of NF-κB dependent hypoxia inducible gene signature in different cell types.

A. RNA-seq (n=3) in the indicated cell types cultured at 21% oxygen (control) or exposed to 24 h 1% oxygen (hypoxia). **B.** Volcano plots displaying differential expression analysis comparing 24h hypoxia to control from RNA-seq datasets in the indicated cell lines. **C.** Overlap of hypoxia inducible DEGs identified in different cell lines' RNA-seq datasets with NF-κB dependent hypoxia inducible DEGs identified in HeLa RNA-seq experiment following siRNA depletion of individual NF-κB subunits exposed or not to 24 h hypoxia. Percentage of NF-κB dependent hypoxia inducible DEGs are displayed **D.** Overlap of hypoxia inducible DEGs identified in different cell lines' RNA-seq datasets with the Gilmore laboratory's NF-κB target genes. Percentage of NF-κB target genes are displayed.

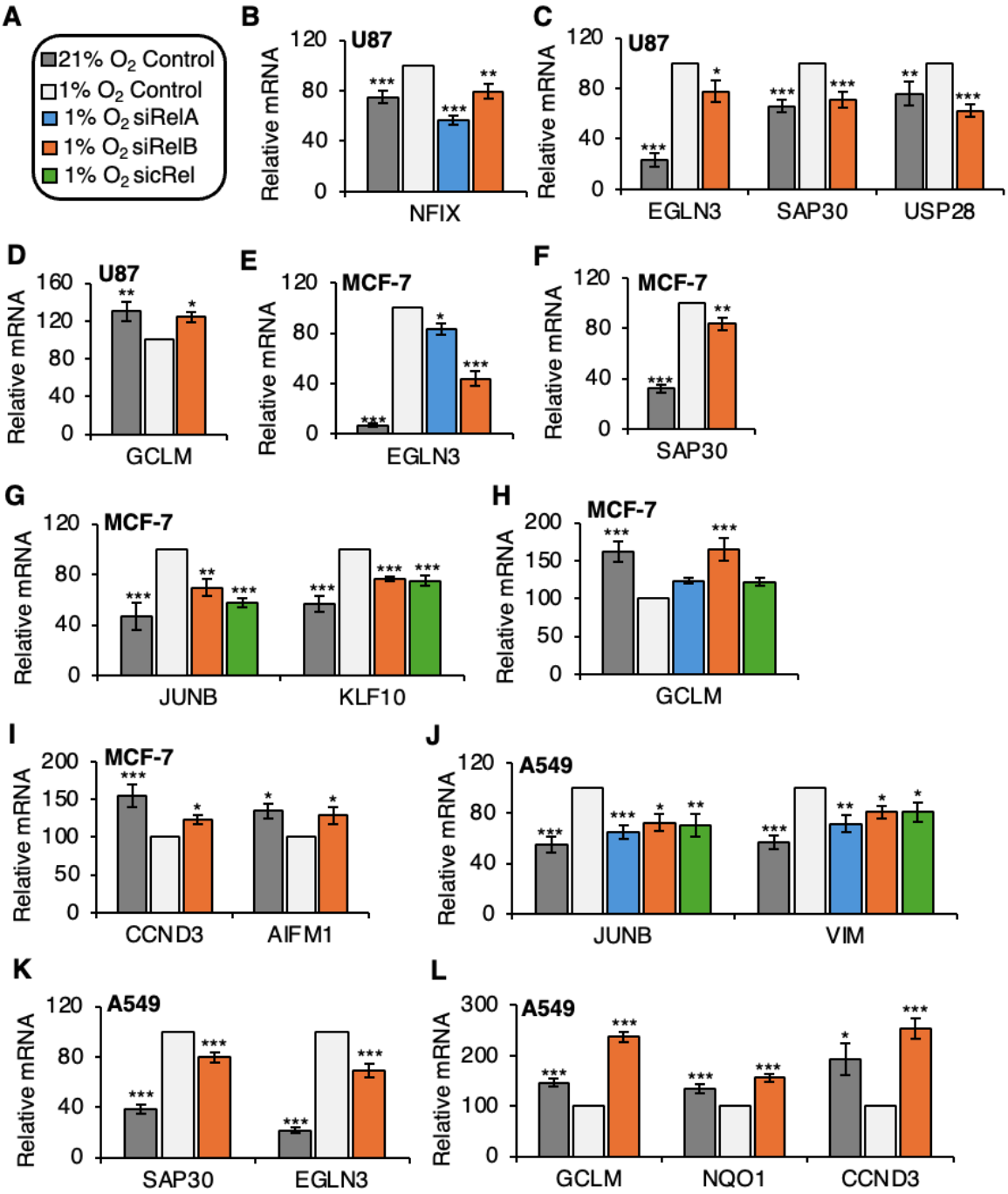

Figure 5. Analysis of hypoxia inducible NF-κB-dependent genes across various cell backgrounds.
A. Key for qPCR analysis graphs. **B-C.** Hypoxia upregulated NF-κB-dependent genes in U87 cells. **D.** Hypoxia downregulated NF-κB-dependent genes in U87 cells. **E-G.** Hypoxia upregulated NF-κB-dependent genes in

MCF-7 cells. **H-I.** Hypoxia downregulated NF-*κ*B-dependent genes in MCF-7 cells. **J-K.** Hypoxia upregulated NF-*κ*B-dependent genes in A549 cells. **L.** Hypoxia downregulated NF-*κ*B-dependent genes in A549 cells. Relative mRNA expression levels of the indicated genes were analysed using Actin as a normalising gene for U87 and MCF-7 cell lines (**B-I**), and 18S for A549 cells (**J-L**). Graphs show mean (n=3) ± SEM, * $P < 0.05$, ** $P < 0.01$, *** $P < 0.001$. Statistical significance was determined via one-way ANOVA with post-hoc Dunnett's test.

NF-*κ*B is important for hypoxia induced cellular responses.

Given the extent of NF-κB contribution to the transcriptional response to hypoxia (35% of activated and 62% of repressed genes), we next determined if any of the cellular responses to hypoxia were altered in the absence of NF-κB subunits. Pathway analysis of the gene repressed in hypoxia that depend on NF-κB indicated Reactive Oxygen Species (ROS) and Oxidative phosphorylation as two of the main hallmarks altered. To validate this at the cellular level, we measured ROS production using a molecular dye (CellRox), that we have previously used to demonstrate that hypoxia induces ROS generation in these cells (Batie *et al*, 2019). As expected, hypoxia exposure resulted in a significant increase in ROS detected by this approach (Figure 6A-B). Importantly, depletion of RelA, and to a lesser extent RelB and cRel, reduced the ROS levels generated in hypoxia (Figure 6A-B). As this specific ROS probe, primarily detects superoxide in cells (McBee *et al*, 2017), we investigated genes specifically associated with reducing superoxide levels in cells. One such genes is superoxide dismutase 1, SOD1. Although, we could not demonstrate a statistical change in levels of mRNA for SOD1 when NF-κB subunits were depleted in hypoxia (Sup. Figure S4G-H), western blot analysis confirmed that hypoxia does lead to reduced SOD1 expression (Figure 6C-D), and that RelB, and to lesser extent cRel and RelA, relieved this repression when depleted (Figure 6C-D). These results suggest that ROS generation in hypoxia require NF-κB via a mechanism that partially requires SOD1 reduction.

Similarly, we investigated a panel of proteins involved in oxidative phosphorylation (Figure 7). This panel contained antibodies for proteins such as ATP Synthase F1 subunit alpha (ATP5A); Ubiquinol-cytochrome C reductase core protein 2 (UQCRC2), Succinate Dehydrogenase subunit B (SDHB) and Isocitrate Dehydrogenase 1 (IDH1). We confirmed that hypoxia led to reductions in several proteins represented in this panel, such as UQCRC2 and IDH1 (Figure 7A-B). Slight reduction was also observed in ATP5A but this was not statistically significant. Hypoxia also led to increases in SDHB, but depletion of NF-κB had no impact on this increase. Depletion of NF-κB led to reversal of the protein levels to those of normoxia or slightly above for IDH1 and ATP5A and very slight increases for UQCRC2 (Figure 7A-B). These data support our RNA-seq analysis, where oxidative phosphorylation was a hallmark significant repressed in hypoxia, dependent on NF-κB presence (Figure 2G).

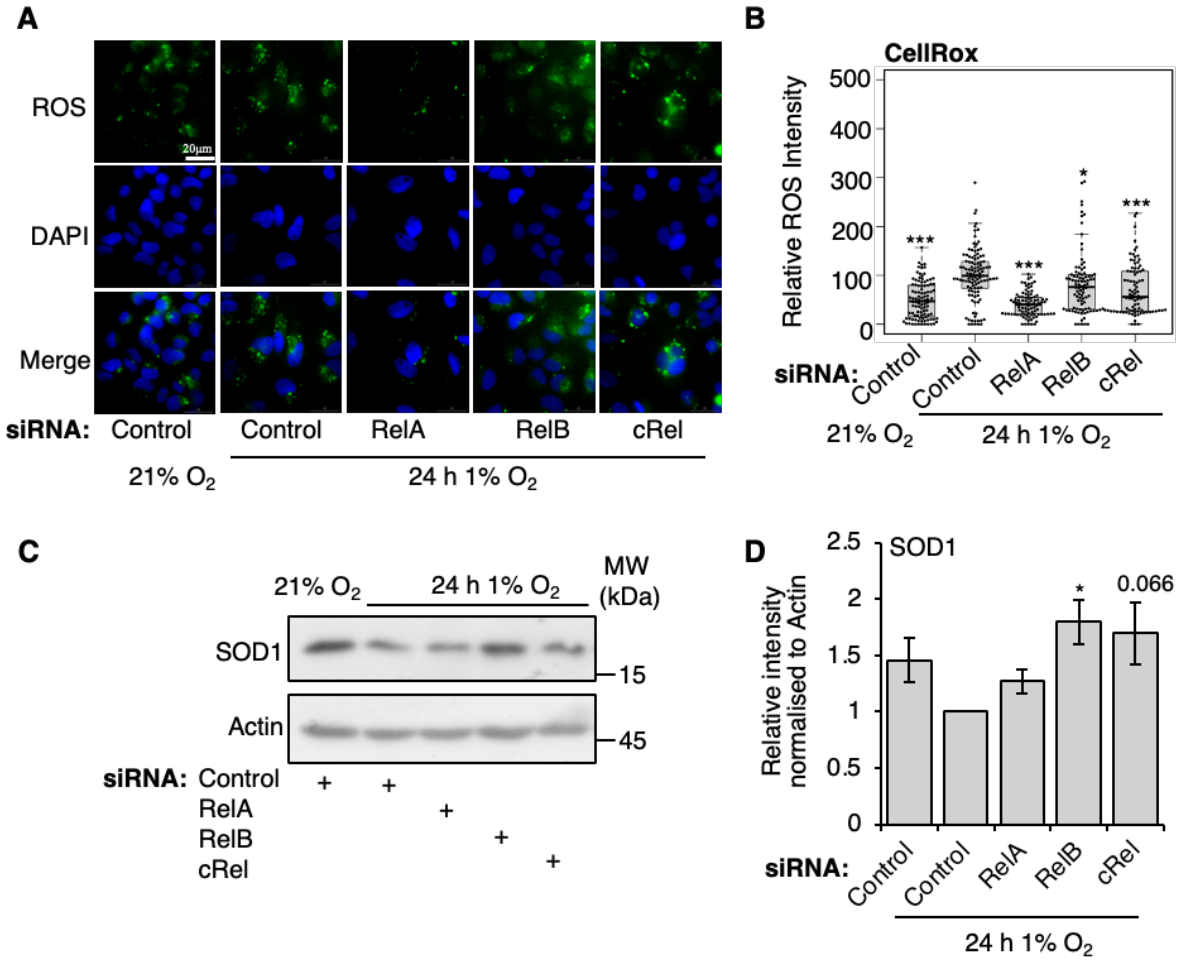

Figure 6. NF-κB is required for ROS generation in hypoxia.

A. Cellular ROS measurements using CellRox staining and immunofluorescence analysis in HeLa cells, cultured at 21% oxygen (control) or 24 h 1% oxygen (hypoxia), transfected with control siRNA or RelA, RelB or cRel siRNAs. Representative images from 3 independent experiments are shown. **B.** Quantification of relative ROS signal in individual cells, mean (n=3) ± SEM, * $P < 0.05$, ** $P < 0.01$, *** $P < 0.001$. Statistical significance was determined via one-way ANOVA with post-hoc Dunnett's test. **C.** Immunoblot analysis of the indicated protein in HeLa cells exposed or not to 1% oxygen for 24 h, with siRNA transfection of control, RelA, RelB or cRel. **D.** Signal intensity normalised to actin (mean n=3, ± SEM) from immunoblot analysis in (**C**). * $P < 0.05$, ** $P < 0.01$, *** $P < 0.001$. Statistical significance was determined via one-way ANOVA with post-hoc Dunnett's test.

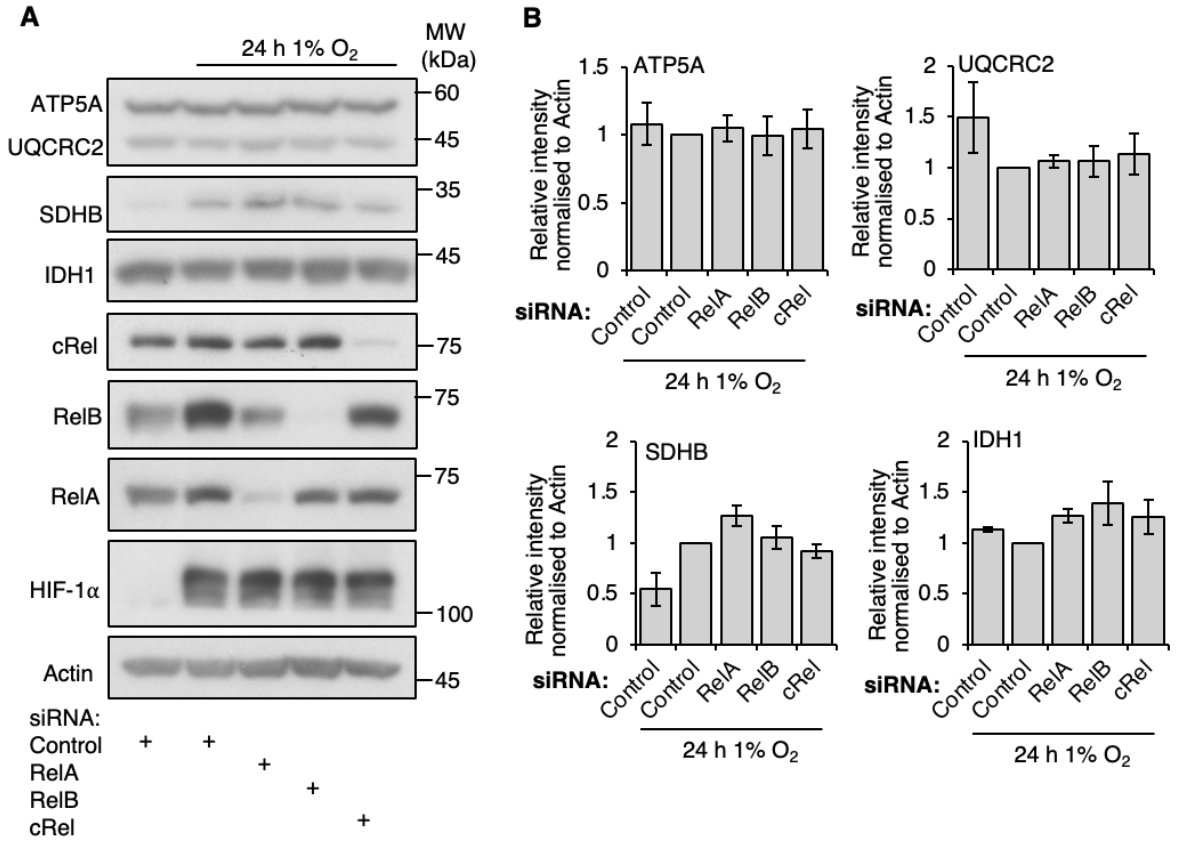

Figure 7. NF-κB is required for expression of oxidative phosphorylation related proteins in hypoxia. **A.** Immunoblot analysis of the indicated proteins in HeLa cells cultured at 21% oxygen (control) or 24 h 1% oxygen (hypoxia), transfected with control siRNA or RelA, RelB or cRel siRNAs. Representative images from 3 independent experiments are shown. **B.** Signal intensity normalised to actin (mean n=3, ± SEM) from immunoblot analysis in (**A**). * $P < 0.05$, ** $P < 0.01$, *** $P < 0.001$. Statistical significance was determined via one-way ANOVA with post-hoc Dunnett's test.

Discussion

Here, we have investigated the contribution of NF-κB towards the transcriptional response in hypoxia. NF-κB pathway activation in hypoxia has been well documented across cells, tissues and organisms (Bandarra *et al*, 2014; Cummins & Taylor, 2005; D'Ignazio & Rocha, 2016; Van Welden *et al*, 2017). While the exact mechanism of activation may depend on the system and timing of the investigation, there is no doubt NF-κB is part of the cell's response to hypoxia. However, to what extent NF-κB contributes to the cell's transcriptional response to hypoxia was not known. Most of the current knowledge in hypoxia is based on the role of HIFs, whose role as a master regulator of the transcriptional response is well established from direct chromatin binding (Batie *et al*, 2022), to conserved list of genes consistently induced in hypoxia (Puente-Santamaria *et al.*, 2022). Individual depletion of Rel subunits, reveals that NF-κB is required for 35% of all hypoxia induced genes but strikingly is required for over 60% of all hypoxia repressed genes. Interestingly, RelB importance is as prevalent as RelA, something previously not appreciated in the response to hypoxia, as almost no studies

have investigated RelB's role in hypoxia. Interestingly, these signatures are more widely regulated across cell types than validated NF-κB targets, suggesting that perhaps NF-κB-dependent genes in hypoxia are different from standard cytokine induced ones. In addition. analysis of ChIP-Atlas database, confirmed that 80% of the genes we have identified to be NF-κB dependent have NF-κB subunits bound to them, indicating a role for direct gene regulation by NF-κB. Further analysis performing ChIP-seq or CUT&RUN in hypoxia for NF-κB subunits would be able to verify this hypothesis and help distinguish between direct and indirect regulation of genes by NF-κB in hypoxia. It is also important to acknowledge that NF-κB is critical to maintain HIF gene expression in different cells and organisms (D'Ignazio & Rocha, 2016; Kenneth *et al*, 2009; Rius *et al*, 2008; van Uden *et al*, 2008; van Uden *et al*, 2011). As such, for genes known to be HIF-dependent, NF-κB's function could be indirect. This is also supported by the analysis of HIF ChIP-seq data where there was a positive correlation of HIF binding and upregulation of genes that are also NF-κB dependent.

Unlike HIF, NF-κB is able to actively repress genes (Burkhart *et al*, 2005; Campbell *et al*, 2004; Elsharkawy *et al*, 2010; Saha *et al*, 2008) and it does this by actively recruiting repressor proteins such as HDACs (Elsharkawy *et al.*, 2010), or by engaging with repressor complexes such as EZH2 directly (Dardis *et al*, 2023) or via nuclear sumoylated-IκBα (Culver *et al.*, 2010). The extent of NF-κB contribution to the transcriptional response to hypoxia is thus quite clear and highlights the importance of NF-κB under such a critical stimulus. In the future studies it would be ideal to investigate if hypoxia induces nuclear IκBα that is sumoylated. Interestingly, analysis of available RNA-seq data from cells depleted of SENP3, a sumo protease highlighted that modulation of sumoylation by this enzyme has significant overlaps with hypoxia dependent NF-κB gene signatures (Sup. Figure S10), suggesting that inhibition of SENPs in hypoxia (Culver *et al.*, 2010; Kunz *et al*, 2016) is another mechanism able to control NF-κB.

The hallmark signatures for hypoxia repressed genes controlled by NF-κB were ROS signalling and Oxidative Phosphorylation. Although distinct, these signatures are intrinsically linked in hypoxia (Hamanaka & Chandel, 2010; Solaini *et al*, 2010). Given the reduction in oxygen, mitochondria are considered one of the sources of ROS due to alteration in the electron transport chain activity (Kracht *et al*, 2020; Solaini *et al.*, 2010). Furthermore, reducing the expression of genes associated with oxidative phosphorylation in time of oxygen deficiency is a cost-effective mechanism to conserve energy (Kracht *et al.*, 2020). Although technically we are unable to measure oxygen consumption in hypoxia, we could determine that several proteins associated with this function were reduced in hypoxia and that NF-κB depletion reversed this repression. This might be, in the long term, detrimental for the cell, as cell death could be a consequence of prolonged NF-κB depletion in hypoxia.

NF-κB has been previously shown to translocate to mitochondria as well (Ivanova & Perkins, 2019), a process important for ROS generation. Our study has further added to this evidence, in unbiased manner,

and reproduced NF-κB's role in generation of ROS in response to hypoxia. ROS's role in hypoxia is multifaceted (Alva *et al*, 2024; Hamanaka & Chandel, 2010), and hence it contributes not only to pathology but is also used as a signalling molecule. However, these roles seem to be quite cell type specific (Alva *et al.*, 2024). Overall, our study has revealed the importance of NF-κB in the control of the transcriptional response to hypoxia. Surprisingly, NF-κB's main contribution is associated with transcriptional repression. Although very important (Batie *et al.*, 2018; Cavadas *et al.*, 2017), the knowledge around this aspect of gene regulation in hypoxia is not well understood, so this work begins to address this part of the gene expression profile.

Data Availability

The HeLa NF-κB depletion in response to hypoxia RNA-seq dataset is accessible at NCBI GEO: GSE260616. The SKNAS hypoxia stimulation RNA-seq dataset is accessible at NCBI GEO: GSE284326.

Acknowledgements

We would like to acknowledge the members of Rocha and Kenneth labs for helpful discussions and the member of the hypoxia and NF-kappaB community for sharing their RNA-seq data. We thank Dr. Marco Sciacovelli (University of Liverpool) for providing the OxPhos antibody set and Dr. Dom Byrne for the SOD1 antibody. This work was funded by a Wellcome trust collaborator grant to SR (206293/Z/17/Z) and the University of Liverpool, CSK is supported by a fellowship from the Royal College of Surgeons in England (RCSEng), a Tung Postgraduate fellowship and Alder Hey Children's Charity. NKS is supported by Worldwide Cancer Research [grant number 24-0353].

Competing interests

The authors declare no competing interests.

Author contributions

D.S. and S.R conceptualised and oversaw the project. D.S., M. B. and C. S. K. performed the RNA seq analysis. D.S. performed most of the experiments and analysed the data associated with it. D.S, M.B., NSK and S.R. wrote the manuscript. SR obtained the funding.

References:

Adhikari A, Xu M, Chen ZJ (2007) Ubiquitin-mediated activation of TAK1 and IKK. *Oncogene* 26: 3214-3226
Al-Anazi A, Parhar R, Saleh S, Al-Hijailan R, Inglis A, Al-Jufan M, Bazzi M, Hashmi S, Conca W, Collison K *et al* (2018) Data on hypoxia-induced VEGF, leptin and NF-kB p65 expression. *Data Brief* 21: 2395-2397
Allan C, Burel JM, Moore J, Blackburn C, Linkert M, Loynton S, Macdonald D, Moore WJ, Neves C, Patterson A *et al* (2012) OMERO: flexible, model-driven data management for experimental biology. *Nat Methods* 9: 245-253
Almaden JV, Liu YC, Yang E, Otero DC, Birnbaum H, Davis-Turak J, Asagiri M, David M, Goldrath AW, Hoffmann A (2016) B-cell survival and development controlled by the coordination of NF-kappaB family members RelB and cRel. *Blood* 127: 1276-1286
Alva R, Wiebe JE, Stuart JA (2024) Revisiting reactive oxygen species production in hypoxia. *Pflugers Arch* 476: 1423-1444
An J, Rettig MB (2005) Mechanism of von Hippel-Lindau protein-mediated suppression of nuclear factor kappa B activity. *Mol Cell Biol* 25: 7546-7556
Bandarra D, Biddlestone J, Mudie S, Muller HA, Rocha S (2014) Hypoxia activates IKK-NF-kappaB and the immune response in Drosophila melanogaster. *Biosci Rep* 34
Batie M, Del Peso L, Rocha S (2018) Hypoxia and Chromatin: A Focus on Transcriptional Repression Mechanisms. *Biomedicines* 6
Batie M, Frost J, Frost M, Wilson JW, Schofield P, Rocha S (2019) Hypoxia induces rapid changes to histone methylation and reprograms chromatin. *Science* 363: 1222-1226
Batie M, Kenneth NS, Rocha S (2022) Systems approaches to understand oxygen sensing: how multi-omics has driven advances in understanding oxygen-based signalling. *Biochem J* 479: 245-257
Bruegge K, Jelkmann W, Metzen E (2007) Hydroxylation of hypoxia-inducible transcription factors and chemical compounds targeting the HIF-alpha hydroxylases. *Curr Med Chem* 14: 1853-1862
Burkhart BA, Hebbar PB, Trotter KW, Archer TK (2005) Chromatin-dependent E1A activity modulates NF-kappaB RelA-mediated repression of glucocorticoid receptor-dependent transcription. *J Biol Chem* 280: 6349-6358
Campbell KJ, Rocha S, Perkins ND (2004) Active repression of antiapoptotic gene expression by RelA(p65) NF-kappa B. *Mol Cell* 13: 853-865
Cavadas MAS, Cheong A, Taylor CT (2017) The regulation of transcriptional repression in hypoxia. *Exp Cell Res* 356: 173-181
Culver C, Sundqvist A, Mudie S, Melvin A, Xirodimas D, Rocha S (2010) Mechanism of hypoxia-induced NF-kappaB. *Mol Cell Biol* 30: 4901-4921
Cummins EP, Taylor CT (2005) Hypoxia-responsive transcription factors. *Pflugers Arch* 450: 363-371
D'Ignazio L, Batie M, Rocha S (2017) Hypoxia and Inflammation in Cancer, Focus on HIF and NF-kappaB. *Biomedicines* 5
D'Ignazio L, Rocha S (2016) Hypoxia Induced NF-kappaB. *Cells* 5
Dardis GJ, Wang J, Simon JM, Wang GG, Baldwin AS (2023) An EZH2-NF-kappaB regulatory axis drives expression of pro-oncogenic gene signatures in triple negative breast cancer. *iScience* 26: 107115
Dobin A, Davis CA, Schlesinger F, Drenkow J, Zaleski C, Jha S, Batut P, Chaisson M, Gingeras TR (2013) STAR: ultrafast universal RNA-seq aligner. *Bioinformatics* 29: 15-21

Durinck S, Moreau Y, Kasprzyk A, Davis S, De Moor B, Brazma A, Huber W (2005) BioMart and Bioconductor: a powerful link between biological databases and microarray data analysis. *Bioinformatics* 21: 3439-3440
Edgar R, Domrachev M, Lash AE (2002) Gene Expression Omnibus: NCBI gene expression and hybridization array data repository. *Nucleic Acids Res* 30: 207-210
Elsharkawy AM, Oakley F, Lin F, Packham G, Mann DA, Mann J (2010) The NF-kappaB p50:p50:HDAC-1 repressor complex orchestrates transcriptional inhibition of multiple pro-inflammatory genes. *J Hepatol* 53: 519-527
Fandrey J, Gorr TA, Gassmann M (2006) Regulating cellular oxygen sensing by hydroxylation. *Cardiovasc Res* 71: 642-651
Gerondakis S, Siebenlist U (2010) Roles of the NF-kappaB pathway in lymphocyte development and function. *Cold Spring Harb Perspect Biol* 2: a000182
Hamanaka RB, Chandel NS (2010) Mitochondrial reactive oxygen species regulate cellular signaling and dictate biological outcomes. *Trends Biochem Sci* 35: 505-513
Heinz S, Benner C, Spann N, Bertolino E, Lin YC, Laslo P, Cheng JX, Murre C, Singh H, Glass CK (2010) Simple combinations of lineage-determining transcription factors prime cis-regulatory elements required for macrophage and B cell identities. *Mol Cell* 38: 576-589
Iqbal AD, C.; Metge, F.; Rosskopp, D.; Boucas, J. (2021) Flaski.
Ivanova IG, Perkins ND (2019) Hypoxia induces rapid, STAT3 and ROS dependent, mitochondrial translocation of RelA(p65) and IkappaBalpha. *Biosci Rep* 39
Kaelin WG, Jr., Ratcliffe PJ (2008) Oxygen sensing by metazoans: the central role of the HIF hydroxylase pathway. *Mol Cell* 30: 393-402
Kenneth NS, Mudie S, van Uden P, Rocha S (2009) SWI/SNF regulates the cellular response to hypoxia. *J Biol Chem* 284: 4123-4131
Kenneth NS, Rocha S (2008) Regulation of gene expression by hypoxia. *Biochem J* 414: 19-29
Kracht M, Muller-Ladner U, Schmitz ML (2020) Mutual regulation of metabolic processes and proinflammatory NF-kappaB signaling. *J Allergy Clin Immunol* 146: 694-705
Kunz K, Wagner K, Mendler L, Holper S, Dehne N, Muller S (2016) SUMO Signaling by Hypoxic Inactivation of SUMO-Specific Isopeptidases. *Cell Rep* 16: 3075-3086
Liao Y, Smyth GK, Shi W (2013) The Subread aligner: fast, accurate and scalable read mapping by seed-and-vote. *Nucleic Acids Res* 41: e108
Liao Y, Wang J, Jaehnig EJ, Shi Z, Zhang B (2019) WebGestalt 2019: gene set analysis toolkit with revamped UIs and APIs. *Nucleic Acids Res* 47: W199-W205
Liberzon A, Birger C, Thorvaldsdottir H, Ghandi M, Mesirov JP, Tamayo P (2015) The Molecular Signatures Database (MSigDB) hallmark gene set collection. *Cell Syst* 1: 417-425
Liu T, Zhang L, Joo D, Sun SC (2017) NF-kappaB signaling in inflammation. *Signal Transduct Target Ther* 2: 17023-
Love MI, Huber W, Anders S (2014) Moderated estimation of fold change and dispersion for RNA-seq data with DESeq2. *Genome Biol* 15: 550
McBee ME, Chionh YH, Sharaf ML, Ho P, Cai MW, Dedon PC (2017) Production of Superoxide in Bacteria Is Stress- and Cell State-Dependent: A Gating-Optimized Flow Cytometry Method that Minimizes ROS Measurement Artifacts with Fluorescent Dyes. *Front Microbiol* 8: 459
Melvin A, Mudie S, Rocha S (2011) Further insights into the mechanism of hypoxia-induced NFkappaB. [corrected]. *Cell Cycle* 10: 879-882
Ortmann BM, Burrows N, Lobb IT, Arnaiz E, Wit N, Bailey PSJ, Jordon LH, Lombardi O, Penalver A, McCaffrey J *et al* (2021) The HIF complex recruits the histone methyltransferase SET1B to activate specific hypoxia-inducible genes. *Nat Genet* 53: 1022-1035

Patel H, Zaghloul N, Lin K, Liu SF, Miller EJ, Ahmed M (2017) Hypoxia-induced activation of specific members of the NF-kB family and its relevance to pulmonary vascular remodeling. *Int J Biochem Cell Biol* 92: 141-147
Perkins ND (2007) Integrating cell-signalling pathways with NF-kappaB and IKK function. *Nat Rev Mol Cell Biol* 8: 49-62
Perkins ND, Gilmore TD (2006) Good cop, bad cop: the different faces of NF-kappaB. *Cell Death Differ* 13: 759-772
Prescott JA, Mitchell JP, Cook SJ (2021) Inhibitory feedback control of NF-kappaB signalling in health and disease. *Biochem J* 478: 2619-2664
Puente-Santamaria L, Sanchez-Gonzalez L, Pescador N, Martinez-Costa O, Ramos-Ruiz R, Del Peso L (2022) Formal Meta-Analysis of Hypoxic Gene Expression Profiles Reveals a Universal Gene Signature. *Biomedicines* 10
Qin ZH, Tao LY, Chen X (2007) Dual roles of NF-kappaB in cell survival and implications of NF-kappaB inhibitors in neuroprotective therapy. *Acta Pharmacol Sin* 28: 1859-1872
Rius J, Guma M, Schachtrup C, Akassoglou K, Zinkernagel AS, Nizet V, Johnson RS, Haddad GG, Karin M (2008) NF-kappaB links innate immunity to the hypoxic response through transcriptional regulation of HIF-1alpha. *Nature* 453: 807-811
Rocha S (2007) Gene regulation under low oxygen: holding your breath for transcription. *Trends Biochem Sci* 32: 389-397
Saha A, Hammond CE, Trojanowska M, Smolka AJ (2008) Helicobacter pylori-induced H,K-ATPase alpha-subunit gene repression is mediated by NF-kappaB p50 homodimer promoter binding. *Am J Physiol Gastrointest Liver Physiol* 294: G795-807
Solaini G, Baracca A, Lenaz G, Sgarbi G (2010) Hypoxia and mitochondrial oxidative metabolism. *Biochim Biophys Acta* 1797: 1171-1177
Subramanian A, Tamayo P, Mootha VK, Mukherjee S, Ebert BL, Gillette MA, Paulovich A, Pomeroy SL, Golub TR, Lander ES *et al* (2005) Gene set enrichment analysis: a knowledge-based approach for interpreting genome-wide expression profiles. *Proc Natl Acad Sci U S A* 102: 15545-15550
Tian B, Nowak DE, Brasier AR (2005) A TNF-induced gene expression program under oscillatory NF-kappaB control. *BMC Genomics* 6: 137
van Uden P, Kenneth NS, Rocha S (2008) Regulation of hypoxia-inducible factor-1alpha by NF-kappaB. *Biochem J* 412: 477-484
van Uden P, Kenneth NS, Webster R, Muller HA, Mudie S, Rocha S (2011) Evolutionary conserved regulation of HIF-1beta by NF-kappaB. *PLoS Genet* 7: e1001285
Van Welden S, Selfridge AC, Hindryckx P (2017) Intestinal hypoxia and hypoxia-induced signalling as therapeutic targets for IBD. *Nat Rev Gastroenterol Hepatol* 14: 596-611
Volcic M, Karl S, Baumann B, Salles D, Daniel P, Fulda S, Wiesmuller L (2012) NF-kappaB regulates DNA double-strand break repair in conjunction with BRCA1-CtIP complexes. *Nucleic Acids Res* 40: 181-195
Wilson JW, Shakir D, Batie M, Frost M, Rocha S (2020) Oxygen-sensing mechanisms in cells. *FEBS J* 287: 3888-3906
Xia ZB, Meng FR, Fang YX, Wu X, Zhang CW, Liu Y, Liu D, Li GQ, Feng FB, Qiu HY (2018) Inhibition of NF-kappaB signaling pathway induces apoptosis and suppresses proliferation and angiogenesis of human fibroblast-like synovial cells in rheumatoid arthritis. *Medicine (Baltimore)* 97: e10920
Xie H, Simon MC (2017) Oxygen availability and metabolic reprogramming in cancer. *J Biol Chem* 292: 16825-16832

Xu RX, Liu RY, Wu CM, Zhao YS, Li Y, Yao YQ, Xu YH (2015) DNA damage-induced NF-kappaB activation in human glioblastoma cells promotes miR-181b expression and cell proliferation. *Cell Physiol Biochem* 35: 913-925
Zhou H, Feng W, Yu J, Shafiq TA, Paulo JA, Zhang J, Luo Z, Gygi SP, Moazed D (2023) SENP3 and USP7 regulate Polycomb-rixosome interactions and silencing functions. *Cell Rep* 42: 112339
Zou Z, Ohta T, Oki S (2024) ChIP-Atlas 3.0: a data-mining suite to explore chromosome architecture together with large-scale regulome data. *Nucleic Acids Res* 52: W45-W53